

# Stokes polarimeter using vector diffractive optical elements

Angela Soria-Garcia<sup>a,\*</sup>, Jesus del Hoyo<sup>a</sup>, Luis Miguel Sanchez-Brea<sup>a</sup>, Veronica Pastor-Villarrubia<sup>a,b</sup>, Veronica Gonzalez-Fernandez<sup>b</sup>, Mahmoud H.Elshorbagy<sup>c</sup>, and Javier Alda<sup>b</sup>

<sup>a</sup>Applied Optics Complutense Group, Optics Department, Faculty of Physics, Universidad Complutense de Madrid, Plaza de las Ciencias 1, 28040, Madrid, Spain

<sup>b</sup>Applied Optics Complutense Group, Optics Department, Faculty of Optics and Optometry, Universidad Complutense de Madrid, C/ Arcos de Jalón 118, 28037, Madrid, Spain

<sup>c</sup>Faculty of Science, Minia University, 61519 El-Minya, Egypt

## ABSTRACT

The characterization of polarimetric properties of light is very important for many applications. Most commercial devices require several sequential measurements to determine the Stokes vector compromising real-time characterization. To solve this limitation, we have designed a device that uses a Vectorial Diffractive Optical Element (VDOE) to determine the Stokes vector in a single measurement. The aperture of the VDOE is angularly sectorized. Each sector contains a Fresnel Zone Plate (FZP) which focus the incoming light in several separate foci, one per sector. Also, the sectors have different polarization properties (i.e., different Mueller matrices). This allows determining the Stokes vector from the intensities of the different foci, which are collected by a dedicated photodetector array or a camera. Our simulations identified some error sources of this device as diffractive effects and systematic errors. After a thoughtful analysis, we could determine the incident state with an averaged residual uncertainty of 0.006%. Finally, we manufactured the VDOE using FZPs printed on transparent plastic plus the appropriate commercial polarizers and quarter-waveplates. Our experimental results show an average error of 3.33%, being comparable to existing polarimetric technologies.

**Keywords:** Vector Diffractive Optical Element, Polarimetry, Stokes parameters

## 1. INTRODUCTION

The polarization state of light is a relevant parameter to understand how electromagnetic radiation interacts with the matter. In fact, this property of light is used in many fields as material analysis, chemistry, medicine, defense, remote sensing or biology.<sup>1-3</sup> Mathematically, the polarization state of light can be described with the Jones formalism, which analyzes totally-polarized light, and the Mueller-Stokes formalism, that studies partially-polarized light.<sup>4</sup> Technically, several methods have been proposed to determine the polarization of a beam such as rotating linear retarders or division-of amplitude devices. Regarding to the rotating plates method,<sup>5,6</sup> it is a very common technique that uses a rotating linear retarder followed by a fixed polarizer. The intensity that goes through the system is measured by a photodiode and the Stokes vector of the beam is determined. Trying to remove moving parts, Pockels cells or liquid crystals can be used to measure sequentially the state of polarization.<sup>7</sup> Moreover, no moving real-time devices, as division-of-amplitude technique,<sup>8</sup> can determine the Stokes parameters directly. For example, beam splitters can be used to divide the incoming light into four beams. Then, each beam passes through different polarizing plates and its intensity is measured by a photodiode to determine the Stokes vector. Nevertheless, this procedure entails voluminous elements with strong alignment constrains.

In this work, we propose a Stokes analyzer using a Vector Diffractive Optical Element (VDOE). This device is formed by an amplitude Diffractive Optical Element (DOE) combined with polarizers and quarter-wave plates, which provides the vectorial properties. Classical DOEs usually modulate the amplitude or the phase of a light beam. Nevertheless, as our VDOE, they can also modulate the coherence or the state of polarization.<sup>9,10</sup> The

designed VDOE is sectorized into 6 areas, where each one includes a Fresnel Zone Plate (FZP) and an appropriate combination of a polarizer and, if required, a retardance plate. The light emerging from the VDOE is measured by a photodetector and, using Mueller-Stokes formalism, the Stokes vector of the input light is determined. Therefore, the proposed VDOE allows us to set the polarization state of an input beam in a precise, quick and robust way.<sup>11</sup>

The manuscript is organised as follows. In Section 2, we show the parameters of the VDOE design and we explain how we obtain the Stokes parameters using ideal and non-ideal polarizing elements. In Section 3 we perform a deep analysis of the main error sources of our device and we show how the uncertainty drops when these error sources are taken into account. Then, in Section 4 we carry out an experimental verification of the manufactured VDOE performance. Finally, in Section 5 we summarize the main conclusions of our study.

## 2. STOKES POLARIMETER DESIGN

Let us consider a polarization state given by its Stokes vector

$$\vec{S} = \begin{pmatrix} S_0 \\ S_1 \\ S_2 \\ S_3 \end{pmatrix} = \begin{pmatrix} I_T \\ I_{0^\circ} - I_{90^\circ} \\ I_{45^\circ} - I_{135^\circ} \\ I_{RCP} - I_{LCP} \end{pmatrix}, \quad (1)$$

where  $S_0$  represents the total intensity of the beam,  $S_1$  is calculated by subtracting the horizontally and vertically polarized intensity,  $S_2$  represents the difference between  $45^\circ$  and  $135^\circ$  linearly polarized intensity, and  $S_3$  is obtained by subtracting right-handed and left-handed circularly polarized intensity. With the aim of computing the Stokes vector of a beam quickly and accurately, we propose a Vector Diffractive Optical Element (VDOE) sectorized into six equal zones. Each sector has a decentered Fresnel Zone Plate (FZP), a polarizer and a quarter-wave plate, if required, to produce maximum transmission for linear polarization states orientated at  $0^\circ$ ,  $90^\circ$ ,  $45^\circ$ ,  $135^\circ$  and right-handed and left-handed circular polarization states, respectively. The proposed design is shown in Figure 1. The circular aperture of the device is  $D = 6$  mm and the focal distance of all VDOE FZPs is  $f' = 200$  mm, for the design wavelength of  $\lambda = 0.6328 \mu\text{m}$ . Moreover, we displace  $\Delta r = 1.5$  mm the center of the FZPs with respect to the geometrical center of the device to avoid overlapping between the six foci at the focal plane and analyze their intensity independently.

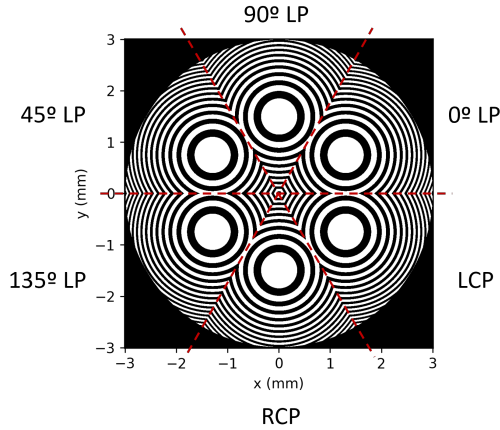


Figure 1. Layout of the sectorized VDOE. Each sector has a FZP with a different polarization matrix. The device contains  $0^\circ$ ,  $90^\circ$ ,  $45^\circ$  and  $135^\circ$  linear polarization states and, right-handed and left-handed circular polarization states.

We use the Mueller-Stokes formalism to characterize the optical behaviour of the VDOE and the vector Rayleigh-Sommerfeld (VRS)<sup>12</sup> approach to determine the intensity distribution at the image plane. We have implemented them with two Python open-source libraries, *Diffractio* for propagation of light<sup>13</sup> and *Py-pol* for

polarization analysis.<sup>14</sup> Using these modules, we have determined the electric field  $\vec{E}(x, y) = [E_x(x, y), E_y(x, y)]$  at the focal plane of the VDOE for the incident polarization states shown in Table 1. The selected input beams generate five bright spots and a dark area which is formed by the sector with the orthogonal analyzer state to the incident light (see Figure 2a). Then, we simulate six circular photodetectors properly placed at each foci position to measure the intensity  $I_k(x, y) = |\vec{E}(x, y)|^2$  of each one and determine the polarization state of the beam using the following expression:

$$\vec{S}_l^{sim} = \begin{pmatrix} S_{0,l}^{sim} \\ S_{1,l}^{sim} \\ S_{2,l}^{sim} \\ S_{3,l}^{sim} \end{pmatrix} = \begin{pmatrix} \frac{1}{3} \sum_{k=1}^6 I_{k,l} \\ I_{1,l} - I_{2,l} \\ I_{3,l} - I_{4,l} \\ I_{5,l} - I_{6,l} \end{pmatrix}, \quad (2)$$

where the super-index <sup>sim</sup> means that the Stokes parameters are obtained through simulation, sub-indexes  $k$  and  $l$  refer to photodetectors and the input state polarization respectively. Moreover, in polarimetry, it is common to use normalized Stokes vector. The first component must be  $S_0 = 1$  and the rest of them are normalized to  $S_0$ . On the other hand, any physically realizable Stokes vector must obey the relation

$$S_0 \geq \sqrt{S_1^2 + S_2^2 + S_3^2}. \quad (3)$$

Therefore, if any Stokes vector does not fulfill this condition, it should be corrected as

$$\vec{s} = \begin{pmatrix} s_0 \\ s_1 \\ s_2 \\ s_3 \end{pmatrix} = \begin{pmatrix} 1 \\ S_1/\alpha \\ S_2/\alpha \\ S_3/\alpha \end{pmatrix}, \quad (4)$$

where  $\alpha = \max(S_0, \sqrt{S_1^2 + S_2^2 + S_3^2})$ . Over this manuscript, we will use normalized and corrected Stokes vector since it is a usual experimental issue that occurs for totally polarized beams. After these corrections, the Stokes parameters measured for the incident polarization states are shown in Table 1 (fourth row).

So far, we have seen how ideal elements perform. However, when Mueller matrices of each VDOE sector are not ideal, the Stokes parameters could not calculate according Equation 2.<sup>15</sup> Let us consider that the real Mueller matrix of sector  $k$  is  $\mathbf{M}_k$ . The intensity that passes through sector  $k$  depends only on the first row of  $\mathbf{M}_k$

$$I_k = \sum_{j=0}^3 m_{0j,k} S_j^{in}. \quad (5)$$

Therefore, the intensities that emerge from the six VDOE sectors can be rearranged to a 6-length vector and they are related to the Stokes parameters through 6x4  $\mathbf{W}$  matrix

$$\vec{I} = \mathbf{W} \vec{S}^{in}. \quad (6)$$

Using the pseudoinverse of  $\mathbf{W}$  matrix, we can obtain the input Stokes vector when non-ideal polarizing plates are used.

### 3. PERFORMANCE ANALYSIS

In this section, we analyze the performance of the VDOE when non-ideal elements are used and we include the study of the two main errors sources, the diffractive effects and the systematic uncertainty. Regarding to diffraction effects, the light passing through sector  $k$  should only focus on the corresponding detector  $k'$ . However, owing to diffraction phenomena, the FZP of each sector focuses the beam on the corresponding detector but also scatters the light to the adjacent ones. Therefore, we quantify the diffraction effects of our VDOE as follows. We illuminate only one sector  $k$  with its highest transmission state or totally depolarized light while blocking the rest

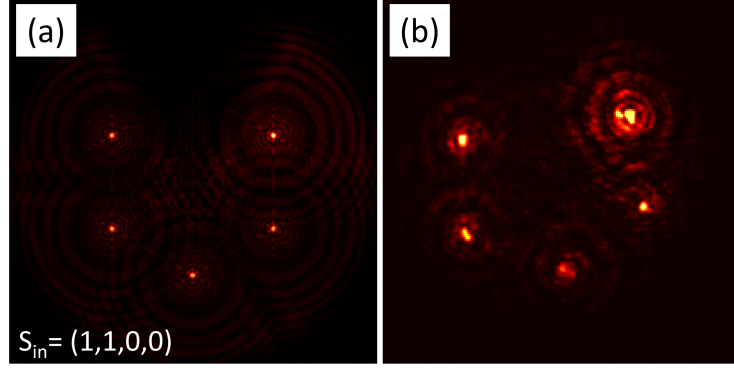


Figure 2. Intensity pattern at the focal plane of the VDOE for an incident beam with horizontal linear polarization. Intensity distribution obtained (a) through simulation and (b) with the experiment.

Table 1. Polarization states of the simulated incident light beam  $\vec{S}_{in}$ . Normalized and corrected Stokes parameters,  $\vec{s}^{sim}$ , measured with the VDOE by simulation. Normalized and corrected Stokes vectors,  $\vec{s}_{C1}^{sim}$ , measured after getting rid of diffraction effects. Normalized and corrected Stokes vectors,  $\vec{s}_{C2}^{sim}$ , measured after removing systematic errors. Uncertainty,  $u(\vec{s}_{C2}^{sim})$ , computed with Equation (8) between corrected,  $\vec{s}_{C2}^{sim}$ , and incident,  $\vec{S}_{in}$ , Stokes vectors.

l	1	2	3	4	5	6
Name	$\vec{S}_{0^\circ}$	$\vec{S}_{90^\circ}$	$\vec{S}_{45^\circ}$	$\vec{S}_{135^\circ}$	$\vec{S}_R$	$\vec{S}_L$
$\vec{S}_{in}$	$\begin{pmatrix} 1 \\ 1 \\ 0 \\ 0 \end{pmatrix}$	$\begin{pmatrix} 1 \\ -1 \\ 0 \\ 0 \end{pmatrix}$	$\begin{pmatrix} 1 \\ 0 \\ 1 \\ 0 \end{pmatrix}$	$\begin{pmatrix} 1 \\ 0 \\ -1 \\ 0 \end{pmatrix}$	$\begin{pmatrix} 1 \\ 0 \\ 0 \\ 1 \end{pmatrix}$	$\begin{pmatrix} 1 \\ 0 \\ 0 \\ -1 \end{pmatrix}$
$\vec{s}^{sim}$	$\begin{pmatrix} 1 \\ 0.989 \\ -0.004 \\ -0.004 \end{pmatrix}$	$\begin{pmatrix} 1 \\ -0.989 \\ 0.004 \\ 0.004 \end{pmatrix}$	$\begin{pmatrix} 1 \\ -0.004 \\ 0.989 \\ -0.004 \end{pmatrix}$	$\begin{pmatrix} 1 \\ 0.004 \\ -0.989 \\ 0.004 \end{pmatrix}$	$\begin{pmatrix} 1 \\ -0.004 \\ -0.004 \\ 0.989 \end{pmatrix}$	$\begin{pmatrix} 1 \\ 0.004 \\ 0.004 \\ -0.989 \end{pmatrix}$
$\vec{s}_{C1}^{sim}$	$\begin{pmatrix} 1 \\ 0.999 \\ -0.003 \\ -0.003 \end{pmatrix}$	$\begin{pmatrix} 1 \\ -0.999 \\ 0.003 \\ 0.003 \end{pmatrix}$	$\begin{pmatrix} 1 \\ -0.003 \\ 0.999 \\ -0.003 \end{pmatrix}$	$\begin{pmatrix} 1 \\ 0.003 \\ -0.999 \\ 0.003 \end{pmatrix}$	$\begin{pmatrix} 1 \\ -0.003 \\ -0.003 \\ 0.999 \end{pmatrix}$	$\begin{pmatrix} 1 \\ 0.003 \\ 0.003 \\ -0.999 \end{pmatrix}$
$\vec{s}_{C2}^{sim}$	$\begin{pmatrix} 1 \\ 1.000 \\ 0.000 \\ 0.000 \end{pmatrix}$	$\begin{pmatrix} 1 \\ -1.000 \\ 0.000 \\ 0.000 \end{pmatrix}$	$\begin{pmatrix} 1 \\ 0.000 \\ 1.000 \\ 0.000 \end{pmatrix}$	$\begin{pmatrix} 1 \\ 0.000 \\ -1.000 \\ 0.000 \end{pmatrix}$	$\begin{pmatrix} 1 \\ 0.000 \\ 0.000 \\ 1.000 \end{pmatrix}$	$\begin{pmatrix} 1 \\ 0.000 \\ 0.000 \\ -1.000 \end{pmatrix}$
$u(\vec{s}_{C2}^{sim})$	0.012%	0.012%	0.006%	0.006%	0.006%	0.006%

of them. Then, we measure the intensity reached to each detector  $k' = 1, \dots, 6$  so that we obtain a 6-component intensity vector. Finally, we repeat this procedure illuminating each sector individually. These intensities are arranged as a  $6 \times 6$  matrix  $\mathbf{D}$  where the element  $D_{kk'}$  represents the intensity received by detector  $k'$  when only sector  $k$  is lit up. The diffraction matrix obtain for our VDOE is the following

$$\mathbf{D} = \begin{pmatrix} 1.0000 & 0.0033 & 0.0005 & 0.0004 & 0.0005 & 0.0033 \\ 0.0033 & 1.0000 & 0.0033 & 0.0005 & 0.0004 & 0.0005 \\ 0.0005 & 0.0033 & 1.0000 & 0.0033 & 0.0005 & 0.0004 \\ 0.0004 & 0.0005 & 0.0033 & 1.0000 & 0.0033 & 0.0005 \\ 0.0005 & 0.0004 & 0.0005 & 0.0033 & 1.0000 & 0.0033 \\ 0.0033 & 0.0005 & 0.0004 & 0.0005 & 0.0033 & 1.0000 \end{pmatrix}. \quad (7)$$

We carry out a first correction of the previous intensity measured using  $\mathbf{D}$  matrix,  $\vec{I}^{C1} = \mathbf{D}^{-1}\vec{I}$ , and we estimate the new Stokes vectors using Equation (2) as we model ideal elements for polarizers and retarders. Table 1 (fifth row) shows the corrected Stokes parameters  $\vec{s}_{C1}^{sim}$ , which are very close to the theoretical ones. Nevertheless, to understand the remaining error, we estimate the Stokes vector for a collection of 250 states that samples the Poincaré sphere regularly.<sup>16</sup> Moreover, to visualize the improvement of our results after corrections, we compute the difference between the measured Stokes vector and the incident one as

$$u(s) = \frac{\sqrt{\sum_{j=0}^3 (s_j - S_j^{in})^2}}{\|\vec{s}\|}, \quad (8)$$

where  $\|\vec{s}\|$  corresponds to the measured Stokes vector module. Figure 3 shows the reduction of the defined error when diffraction effects are removed (Figure 3b respect to Figure 3a). In fact, the maximum uncertainty drops from 2% to 0.6%. From Figures 3a and 3b, we can also see that the error varies uniformly. Therefore, we calculate the uncertainty of each Stokes vector component ( $\Delta S_1, \Delta S_2, \Delta S_3$ ) and we realize that the error has a linear dependence with the Stokes parameters

$$\Delta S_j \approx a_j + b_j S_1 + c_j S_2 + d_j S_3. \quad (9)$$

This systematic uncertainty is caused mainly by the pixel size of our VDOE, that affects the faithful reproduction of the outer zones of the FZPs. We correct this error source as  $\vec{S}_{C2} = \vec{S}_{C1} - \Delta\vec{S}$  and then, we estimate the uncertainty using the corrected Stokes parameters. As we can appreciate in Figure 3c, the maximum uncertainty drops to 0.012%. Finally, in Table 1, we include the new Stokes parameters and the uncertainties for the six original states of polarization. Here, we can see how the system retrieves the input Stokes vector with high fidelity.

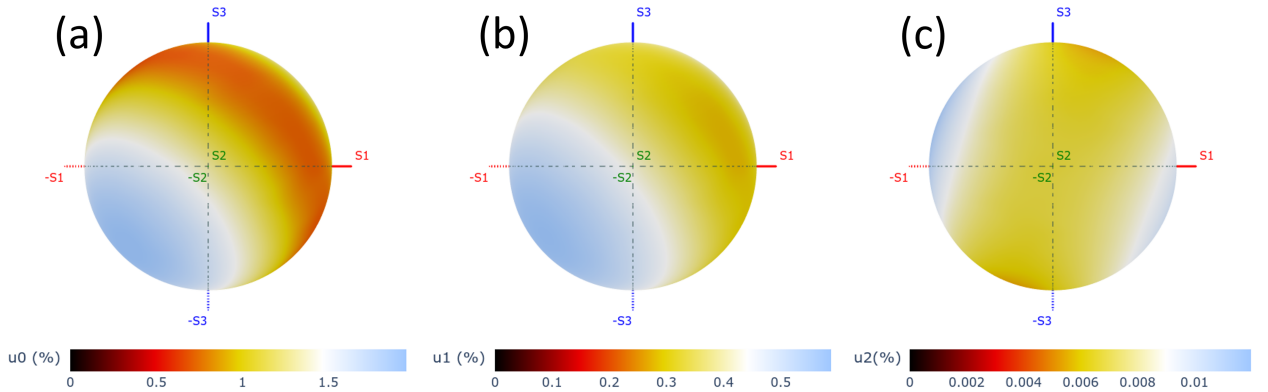


Figure 3. Uncertainty of the Stokes vectors measured with the VDOE over the full Poincaré sphere. Uncertainty obtained (a) before removing any error source, (b) after compensating diffraction effects, and (c) after removing systematic errors.

#### 4. EXPERIMENTAL RESULTS

To validate the proposed Stokes analyzer, we have manufactured the device using an amplitude mask glued to six polyvinyl alcohol-iodine polarizers and two poly-carbonate quarter-wave plates. These plates have been properly orientated in each VDOE sector to generate the designed polarization state. The manufactured device has a clear aperture of  $D = 29$  mm and the focal length of the FZPs is  $f' = 550$  mm. The displacement of the optical axis of the individual FZP with respect to the geometrical center of the VDOE is  $\Delta r = 3.7$  mm. Figure 4 shows the set-up used to analyze the performance of the manufactured VDOE. We use a linearly polarized He-Ne laser ( $\lambda = 0.6328 \mu\text{m}$ ) as a light source, which passes through a beam expander to illuminate the whole aperture of the VDOE. Then, we set the beam polarization to circular using a polarizer (P) and a quarter-wave plate (QW).

Table 2. Generated ( $\vec{S}_g^{\text{exp}}$ ) and analyzed ( $\vec{S}_a^{\text{exp}}$ ) Stokes vectors with the experimental set-up, and uncertainties  $u(\vec{S}_a^{\text{exp}})$  computed using Equation (8).

1	2	3	4	5	6	
Input	$\vec{S}_{0^\circ}^{\text{in}}$	$\vec{S}_{90^\circ}^{\text{in}}$	$\vec{S}_{45^\circ}^{\text{in}}$	$\vec{S}_{135^\circ}^{\text{in}}$	$\vec{S}_R^{\text{in}}$	$\vec{S}_L^{\text{in}}$
$\vec{S}_g^{\text{exp}}$	$\begin{pmatrix} 1 \\ 0.997 \\ 0 \\ -0.083 \end{pmatrix}$	$\begin{pmatrix} 1 \\ -0.984 \\ -0.160 \\ 0.083 \end{pmatrix}$	$\begin{pmatrix} 1 \\ -0.08 \\ 0.993 \\ 0.083 \end{pmatrix}$	$\begin{pmatrix} 1 \\ -0.087 \\ -0.993 \\ 0.083 \end{pmatrix}$	$\begin{pmatrix} 1 \\ 0 \\ 0 \\ 1 \end{pmatrix}$	$\begin{pmatrix} 1 \\ 0 \\ 0 \\ -1 \end{pmatrix}$
$\vec{S}_a^{\text{exp}}$	$\begin{pmatrix} 1 \\ 0.993 \\ -0.062 \\ -0.098 \end{pmatrix}$	$\begin{pmatrix} 1 \\ -0.985 \\ -0.156 \\ 0.079 \end{pmatrix}$	$\begin{pmatrix} 1 \\ -0.084 \\ 0.989 \\ 0.082 \end{pmatrix}$	$\begin{pmatrix} 1 \\ -0.099 \\ -0.995 \\ 0.013 \end{pmatrix}$	$\begin{pmatrix} 1 \\ 0.021 \\ -0.001 \\ 1 \end{pmatrix}$	$\begin{pmatrix} 1 \\ -0.014 \\ 0.007 \\ -1 \end{pmatrix}$
$u(\vec{S}_a^{\text{exp}})$	4.55%	0.45%	0.39%	4.99%	1.48%	1.10%

Next, the light beam goes through a rotated polarizer (R-P) and a rotated quarter-wave plate (R-QW), which can generate any input polarization state. Finally, the polarized beam passes through the VDOE, which focus the light on a CMOS camera. The camera, with 2592x1944 pixels and a pixel size of  $2.2 \times 2.2 \mu\text{m}^2$ , simulates the required photodetectors by integrating the signal on 6 circular areas of  $d = 0.2 \text{ mm}$  and centered at each FZP focal point.

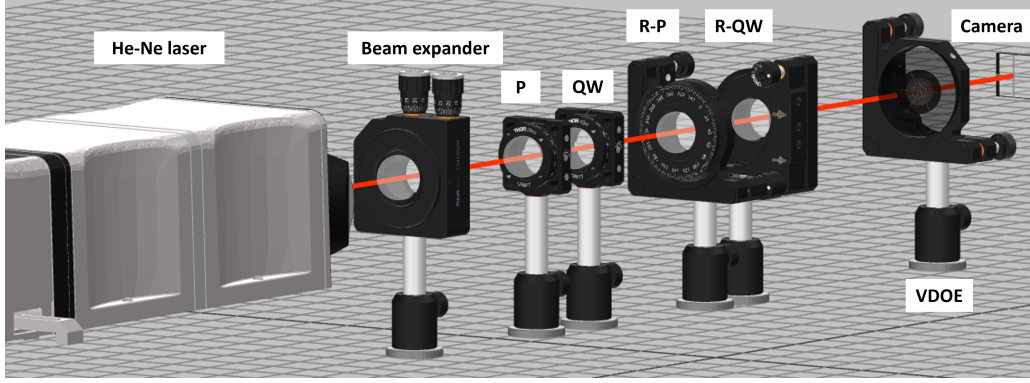


Figure 4. Layout of the set-up used to analyze the performance of the manufactured VDOE. We use an expanded He-Ne laser as light source, whose polarization is fixed to circular using a polarizer (P) and a quarter-wave plate (QW). Then, the beam passes through a motorized polarizer (R-P) and a quarter-wave plate (R-QW) to generate any input polarization state. Finally, the beam goes through the VDOE which focalises the light on the camera.

First, we analyze the performance of the device lighting it up with the six original polarization states. Figure 2b shows an example of the response of the device. It generates 5 bright spots and a dark area at the focal plane since the input light has an orthogonal polarization state to one of the analyzed states of its sectors. Then, we compute the measured Stokes vectors. However, it is important to keep in mind that the polarizers and quarter-wave plates used are not ideal, so we have to measure the Mueller matrix of each sector using the technique described in<sup>17</sup> to determine  $\mathbf{W}$  matrix and, therefore, obtain the experimental Stokes parameters.

Furthermore, using Equation 4 instead of Equation 2 is particularly important for sectors 5 and 6, with which  $S_3$  is evaluated. This happens because these sectors have both polarizer and quarter-wave plates, and the precise adjustment of the elements is not perfect for the experimental realization of the device. Although it was not required in the simulation study, we have also developed a corrected normalization matrix  $\mathbf{N}$  because the light source does not illuminate the device homogeneously ( $\vec{I}' = \mathbf{N}^{-1}\vec{I}$ ). On the other hand, we have also subtracted the diffraction effects and the systematic errors from our experimental data.

Table 2 shows the corrected experimental Stokes parameters with their corresponding errors for the six original polarization states. Moreover, we have computed the uncertainties for 400 input Stokes vectors distributed over

the Poincaré sphere to perform a deep study of our manufactured device. The results obtained are shown at azimuth-ellipticity angle maps of Figure 5a, where we can see that the maximum and mean error are 6.97% and 3.33% respectively. The experimental errors are higher than the simulated ones, which can be attributed to multiple sources as fabrication defects, error in the determination of the Mueller matrices of the polarizers and quarter waveplates,  $\mathbf{N}$  and  $\mathbf{D}$  matrices, and error in the generation of the initial state. Trying to understand the experimental error sources, we repeat the experiment replacing the VDOE by a motorized polarizer and quarter-wave plate. Then, we generate the same 400 input polarization states. For each input state, we rotate the polarizing plates sequentially in order to simulate the polarization of the VDOE sectors. In this case, the intensities are measured by a photodiode instead of a camera. Finally, we estimate the Stokes vector of the input beam applying the corrections mentioned before. The uncertainty of the measured Stokes vector is shown in Figure 5b. The average and maximum discrepancy is 1.47% and 2.76%, respectively. This proves that our experimental set-up (without VDOE) already has non-negligible error due to the uncertainty in the angles of the optical elements and being them no ideal.

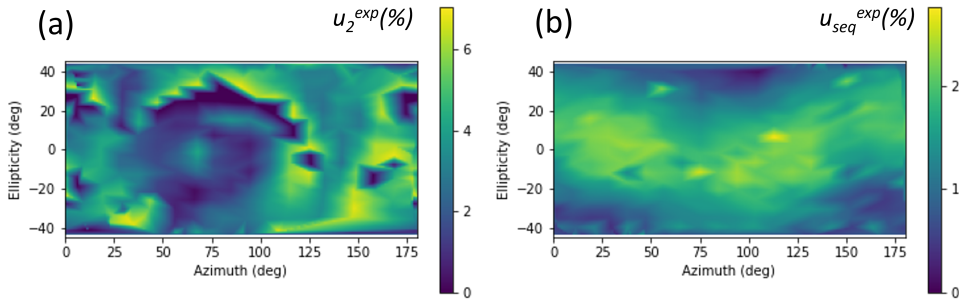


Figure 5. Azimuth-ellipticity angle maps showing the error of the experimental measured Stokes vector using (a) the VDOE and (b) the sequential method (motorized polarizer and quarter-wave plate).

## 5. CONCLUSIONS

We have designed a sectorized Stokes analyzer that allows the real time measurement of the polarization of a light beam. The proposed device is divided into 6 sectors containing an amplitude DOE along with polarizing plates. First, we use as input polarization states those of VDOE sectors, reproducing their Stokes vectors with low uncertainty. We have done a deep numerical analysis of the main error sources of our device. We showed that the diffraction generated by the DOE, deteriorate our results since it scatters the light to undesired positions. Moreover, the VDOE presents systematic errors due to its pixel size. After removing these errors sources, we obtain a maximum uncertainty – for a collection of 250 states distributed over the Poincaré sphere – of 0.012%. Finally, we validate the proposed device by manufacturing it and analyzing its performance. We obtain an average error – for 400 polarization states – of 3.3%, higher than the simulated one. This uncertainty increase is caused by fabrication defects or the uncertainty in the characterization of the polarizing elements of the VDOE. In fact, we compared it with a sequential measurement using rotating plates instead of the VDOE and we still obtain an average discrepancy of 1.47%.

## ACKNOWLEDGMENTS

Authors acknowledge funding from Retos Colaboración 2019 “Teluro” project RTC2019-007113- 3, Ministerio de Economía y Competitividad and the European Union, European funds for regional development; and from Plan Nacional de Investigación from Ministerio de Ciencia e Innovación “Nanorooms” project PID2019-105918GB-I00.

## REFERENCES

- [1] Phan, Q.-H. and Lo, Y.-L., “Stokes-mueller matrix polarimetry system for glucose sensing,” *Optics and Lasers in Engineering* **92**, 120–128 (2017).
- [2] Goldstein, D. H., [*Polarized light*], CRC press (2017).
- [3] Chipman, R. A., Lam, W. S. T., and Young, G., [*Polarized light and optical systems*], Optical sciences and applications of light, CRC Press (2018).
- [4] Rubin, N. A., Shi, Z., and Capasso, F., “Polarization in diffractive optics and metasurfaces,” *Adv. Opt. Photon.* **13**(4), 836–970 (2021).
- [5] Williams, P. A., “Rotating-wave-plate Stokes polarimeter for differential group delay measurements of polarization-mode dispersion,” *Applied Optics* **38**(31), 6508 – 6515 (1999).
- [6] Sabatke, D., Descour, M., Dereniak, E., Sweatt, W., Kemme, S., and Phipps, G., “Optimization of retardance for a complete Stokes polarimeter,” *Optics Letters* **25**(11), 802 – 804 (2000).
- [7] Bueno, J. M., “Polarimetry using liquid-crystal variable retarders: Theory and calibration,” *Journal of Optics A: Pure and Applied Optics* **2**(3), 216 – 222 (2000).
- [8] Azzam, R., “Division-of-amplitude photopolarimeter (DOAP) for the simultaneous measurement of all four stokes parameters of light,” *Optica Acta: International Journal of Optics* **29**(5), 685–689 (1982).
- [9] Soria-Garcia, A., Fantova, J., Blas, A. S., del Hoyo, J., Sanchez-Brea, L. M., Alda, J., Rodriguez, A., and Olaizola, S. M., “Fabrication effects in the optical performance of DOEs engraved with femtosecond lasers,” in [*Optical Fabrication, Testing, and Metrology VII*], **11873**, International Society for Optics and Photonics, SPIE (2021).
- [10] Elshorbagy, M. H., Sanchez-Brea, L. M., Buencuerpo, J., del Hoyo, J., Soria-Garcia, A., Pastor-Villarrubia, V., San-Blas, A., Rodriguez, A., Olaizola, S. M., and Alda, J., “Polarization conversion using customized subwavelength laser-induced periodic surface structures on stainless steel,” *Photon. Res.* **10**(9), 2024–2031 (2022).
- [11] Soria-Garcia, A., del Hoyo, J., Sanchez-Brea, L. M., Pastor-Villarrubia, V., Gonzalez-Fernandez, V., Elshorbagy, M. H., and Alda, J., “Vector diffractive optical element as a full-stokes analyzer,” *Optics & Laser Technology* **163**, 109400 (2023).
- [12] Ye, H., Qiu, C.-W., Huang, K., Teng, J., Luk’yanchuk, B., and Yeo, S. P., “Creation of a longitudinally polarized subwavelength hotspot with an ultra-thin planar lens: Vectorial Rayleigh–Sommerfeld method,” *Laser Physics Letters* **10**(6), 065004 (2013).
- [13] Sanchez-Brea, L. M., “Diffractio: Python library for Diffraction and Interference Optics.” <https://diffractio.readthedocs.io/en/latest/>. (2019).
- [14] del Hoyo, J., Sanchez-Brea, L. M., and Soria-Garcia, A., “Open source library for polarimetric calculations, py\_pol, Proc. SPIE, **1187506**, 3 (2021).” <https://py-pol.readthedocs.io/en/master/>.
- [15] Sabatke, D. S., Descour, M. R., Dereniak, E. L., Sweatt, W. C., Kemme, S. A., and Phipps, G. S., “Optimization of retardance for a complete stokes polarimeter,” *Opt. Lett.* **25**(11), 802–804 (2000).
- [16] Zhou, Y., “Arrangements of points on the sphere,” University of South Florida (1995).
- [17] del Hoyo, J., Sanchez-Brea, L. M., and Gomez-Pedrero, J. A., “High precision calibration method for a four-axis mueller matrix polarimeter,” *Optics and Lasers in Engineering* **132**, 106112 (2020).